SACLANTCEN REPORT
serial no: SR-312

SACLANT UNDERSEA RESEARCH CENTRE REPORT

THE MAGNETIC DIPOLE MOMENT OF RV ALLIANCE

J. Watermann

February 1999

The SACLANT Undersea Research Centre provides the Supreme Allied Commander Atlantic (SACLANT) with scientific and technical assistance under the terms of its NATO charter, which entered into force on 1 February 1963. Without prejudice to this main task — and under the policy direction of SACLANT — the Centre also renders scientific and technical assistance to the individual NATO nations.

SACLANT Undersea Research Centre
Viale San Bartolomeo 400
19138 San Bartolomeo (SP), Italy

tel: +39-0187-5271
fax: +39-0187-524.600

e-mail: library@saclantc.nato.int

NORTH ATLANTIC TREATY ORGANIZATION

The Magnetic Dipole Moment of RV Alliance

J. Watermann

The content of this document pertains to work performed under Project 06-A of the SACLANTCEN Programme of Work. The document has been approved for release by The Director, SACLANTCEN.

Jan L. Spoelstra
Director

intentionally blank page

The Magnetic Dipole Moment of RV Alliance

J. Watermann

Executive Summary:

In September 1998, a four-hour experiment was conducted in order to measure the magnetic signature of the NATO research vessel *Alliance*. DGPS navigation data were recorded with 1 s sampling rate while she sailed along several predefined tracks across an array of tri-axial ocean bottom magnetometers. The magnetic field time series, recorded during the experiment and decimated to 1 s sampling rate, were purged of natural magnetic field variations with the help of a reference magnetometer. A magnetic dipole model was fitted to the data in a least squares sense. As a result, a quantitative model of the horizontal permanent, and induced and the vertical total magnetic dipole moments was derived. The permanent horizontal and the total vertical dipole moments remained constant over the duration of the experiment, but the induced horizontal dipole moment increased steadily and significantly. Instrument effects can be excluded. The induced magnetic dipole moment of the *Alliance* may require a relaxation time of at least several hours in order to adjust to new navigation conditions. If this is valid for other ships, it may have implications for the efficiency of degaussing devices. Further systematic magnetic signature measurements over a longer time interval are needed in order to resolve the problem.

intentionally blank page

The Magnetic Dipole Moment of RV Alliance

J. Watermann

Abstract:

A SACLANTCEN magnetometry sea trial was performed in September 1998 in the northern Tyrrhenian Sea in the vicinity of the Formiche di Grosseto islands. One of the trial objectives concerned the measurement of the magnetic dipole moment of the NATO research vessel *Alliance* with an array of fixed Ocean Bottom Magnetometers. The *Alliance* sailed with constant velocity along three specified tracks in reciprocating directions. The magnetic signature of the *Alliance* was subsequently extracted from the magnetic field data recorded during the experiment. From the magnetic signatures taken from six successive runs, quantitative magnetic dipole models were derived. A comparison between the magnetic signatures obtained from northwestward and southeastward runs yields estimates of the permanent and induced magnetic dipole moments in the horizontal plane. In the vertical direction, only the total magnetic dipole moment can be determined. The positions of the OBMs, uncertain to some extent, were fictitiously varied such that the horizontal components of the permanent magnetic dipole moment and the vertical component of the total dipole moment remained constant during the experiment. The induced horizontal dipole moment tended to increase steadily and monotonically in a northward direction. Explanations of this phenomenon are discussed.

Contents

1

Introduction

The RV *Alliance*, a NATO research ship, bears, like all steel ships, a certain quasi-static magnetization. She has never undergone deperming treatment and does not possess onboard devices for magnetostatic compensation. As her magnetostatic moment, which has never been measured, is expected to be significant, measurements were made during a magnetometry sea trial. As the *Alliance* magnetic signature measurements were not the primary objective of the sea trial, only a few hours were scheduled for the test.

The experiment was unique in the sense that the *Alliance* was not brought into a magnetic ranging facility. Instead, her magnetic signature was observedd under real operating conditions.

The magnetic signature, recorded with an array of fixed **O**cean **B**ottom **M**agneto-meters (OBMs) revealed that the permanent magnetic dipole moment is largely as expected, in direction as well as in strength. The induced magnetic moment, however, appears to not react instantaneously to the geomagnetic field but gradually, with a relaxation time of at least several hours. No straightforward explanation for that effect can be offered.

2

Experimental Setup

During the month of September, 1998, SACLANTCEN operated a two-dimensional array of up to six OBMs northwest of the island of Formica Grande di Grosseto. The island is usually uninhabited and provides for an environment which is free of anthropogenic magnetic noise. From 7-10 September, four of the OBMs were operating simultaneously in a fully autonomous mode. Deployed at bottom depths between 105 and 111 metres, their horizontal spacing ranged from 400 to 1600 m. The OBM's acquired vector time series of the natural ambient magnetic field and of the *Alliance* magnetostatic field when cruising in the test area during the morning of September 8.

Figure 1 shows the Formica Grande sea area with the location of the OBMs and the tracks which were followed by the *Alliance* in reciprocating directions, northwest-bound and southeastbound. It was considered unlikely that the magnetic dipole signature would be measurable beyond a range of some 800 m. It was thus expected that OBM 19 would observe the *Alliance* magnetic field only during the runs along A-B while OBMs 03, 04 and 06 remained free of such signals, and OBMs 03, 04 and 06 would observe the *Alliance* magnetic field (with time overlap) during the runs along G-H and R-S while OBM 19 would remain signal-free. The experiment proved this assumption to be correct.

During the two runs along track A-B, the *Alliance* sailed with nominally 5 kt, and during the other four runs, along the tracks G-H and R-S, with nominally 8 kt. It was possible to reconstruct the navigation of the *Alliance* accurately from a DGPS navigation data acquisition system with 1-s time resolution.

The magnetometers used in the test are of the tri-axial linear core fluxgate type with integrated AC coupling which acts as a highpass filter. They sample variations of the ambient magnetic field at a rate of 2 Hz and store the measurements, accurately time-stamped, in non-volatile solid-state memory. A more comprehensive technical description of the OBMs is given in [1].

3

Data processing

The magnetic field vector time series were low-pass filtered and decimated to a sampling rate of 1 Hz and subsequently transformed into a coordinate system with its x-axis pointing northwest, its y-axis northeast, and its z-axis vertically downward. The Formica Grande lighthouse (projected down to the sea level) was defined as its origin. In this system, the *Alliance* tracks run parallel to the x-axis. The transformation algorithm is described in Annex A of [1].

For a refined inter-sensor alignment, OBM 19 was selected as the reference and the other three OBMs, 03, 04 and 06, were subjected to a further linear time-domain transformation *via* a 3x3 transformation matrix. The matrix coefficients were determined from a trivariate regression analysis between OBM 19 and each of the three other OBMs, using only time intervals undisturbed by human interference. They were selected mainly from the three nights, September 7/8, 8/9 and 9/10.

The regression scheme fits the magnetic field variation, $\mathbf{B}^{NN}$, observed by OBM *NN* ($NN \in \{03, 04, 06\}$), to the magnetic field variation $\mathbf{B}^{19}$, recorded by OBM 19,

$$\begin{pmatrix} B_x^{19}(t) \\ B_y^{19}(t) \\ B_z^{19}(t) \end{pmatrix} = \begin{pmatrix} A_{xx}^{NN} & A_{xy}^{NN} & A_{xz}^{NN} \\ A_{yx}^{NN} & A_{yy}^{NN} & A_{yz}^{NN} \\ A_{zx}^{NN} & A_{zy}^{NN} & A_{zz}^{NN} \end{pmatrix} \cdot \begin{pmatrix} B_x^{NN}(t) \\ B_y^{NN}(t) \\ B_z^{NN}(t) \end{pmatrix} + \begin{pmatrix} \delta B_x(t) \\ \delta B_y(t) \\ \delta B_z(t) \end{pmatrix} \quad (1)$$

The residual vector, $\delta\mathbf{B}$, is that part of the magnetic field that can not be explained through linear regression between the two magnetometers. The coefficients of the regression matrix, (A_{ij}^{NN}), are found by minimizing the sum of the squared error residuals (the elements of the right-most vector on the right hand side of Eq. (1)). This procedure results in magnetic field vectors which we call *optimally aligned and scaled.* The mathematical procedure for computing the coefficients is described in Annex B of [1].

Once a set of matrix coefficients has been determined from each undisturbed time interval, the coefficients are averaged in order to obtain one mean transformation matrix for each of the three magnetometers considered. This matrix is then applied to all data collected by OBM *NN* during the experiment, including those from disturbed intervals. During undisturbed time intervals, the residuals rarely exceeded 0.25 nT which indicates that the ambient magnetic field was relatively uniform.

Once the regression algorithm has been applied, the magnetic field residuals contain only those signals which are not linearly correlated between the magnetometers. In principle, one can then extract the magnetic signature of the *Alliance* from the runs A→B and B→A by comparing the data from OBM 19 with reference measurements from the three other OBMs, and similarly from the runs G→H, H→G, R→S and S→R by using OBM 19 as reference.

The magnetic field of a ship, expected to be recorded by a sensor at a range r, $\mathbf{B}^{(e)}(\mathbf{r})$, can be written in the form

$$\mathbf{B}^{(e)}(\mathbf{r}) = \frac{\mu_0}{4\pi}\left[\frac{3(\mathbf{M}\cdot\hat{\mathbf{r}})\hat{\mathbf{r}} - \mathbf{M}}{r^3} + O\left(\frac{1}{r^4}\right)\right] \tag{2}$$

$\mathbf{M}$ denotes the dipole moment, $\mathbf{r}$ the distance from the vessel's magnetic centre to the magnetometer ($\hat{\mathbf{r}}$ the corresponding unit length vector), and *O(f)* means that the rest of the series, which contains the contribution of higher multipoles, is asymptotically limited by the function f times a constant factor. Obviously, the effect of the higher multipoles decreases rapidly with increasing distance between the ship and the magnetometer. We therefore only attempt to determine the dipole moment of the *Alliance*. Higher multipoles are neglected.

A comparison between the actually measured magnetic signature of the *Alliance* and a signature that would be expected from a moving dipole revealed that the filter effect of the sensor-inherent AC-coupling plays a significant role at the low-frequency end of the passband so that the magnetic field observations differ from the signature of a moving dipole. This necessitated a correction of the observed signals for the sensor frequency response.

Calibration measurements of the sensor response function had been made with two OBMs, covering the frequency range from 1 mHz through 200 mHz (Fig. 2). Based on the results from the calibration measurements, we consider the sensors identical and use a single response function for all sensors and all vector components. The calibration measurements were extrapolated to 0.5 mHz, where an artificial node with half the amplitude and twice the phase of the 1-mHz point was inserted. The calibration data were then converted from amplitude and phase to complex values and polynomials of degree 5, with the decadic logarithm of the frequency as independent variable, were fitted independently to the real and the imaginary parts of the calibration data points.

For each run and each OBM, the time of the nominal **C**losest **P**oint of **A**pproach (CPA) between the *Alliance* and the respective OBM was determined from the navigation parameter files. More precisely, we determined the CPA time between the positions of the GPS reference onboard *Alliance* and the position of the GPS antenna onboard *Manning* at that moment when the magnetometer module was

deployed and hit the sea bottom. We do not expect that the magnetic dipole centre of the *Alliance* coincides with the position of its GPS reference point nor do we expect that the position of the GPS antenna on *Manning* coincided with the position of the OBM once it had settled on the sea bottom.

After having decimated the magnetic field data to a sampling rate of 1 Hz, we formed intervals of 2048 s, roughly centred on the nominal CPA of OBM 19 (for the track A-B) and OBM 03 (for the tracks G-H and R-S), transformed them into the frequency domain, applied the inverse bandpass response function, and transformed them back into the time domain. Figure 3 gives an example of the magnetic field time series collected during the last run of the *Alliance*, R→S, and treated this way. We subsequently extracted intervals of 540 s for the first two runs (at 5 kt speed), and intervals of 320 s for the last four runs (at 8 kt), respectively, all centred on the nominal CPA for each individual OBM. For each interval, we determined a mean speed of the *Alliance* and the distance from the nominal position of the OBM at the corresponding CPA, using the DGPS navigation data (Table 1).

Table 1 *RV Alliance Run Parameters*

Run ID	OBM	Bottom Depth	CPA Time (UTC)	CPA Distance	Speed
B→A	M19	111 m	09:43:09	143 m	2.42 m/s
A→B	M19	111 m	10:28:22	144 m	−2.47 m/s
H→G	M04	105 m	11:04:59	−228 m	4.14 m/s
	M03	105 m	11:06:35	−231 m	4.14 m/s
	M06	106 m	11:08:12	−225 m	4.12 m/s
G→H	M06	106 m	11:36:46	−222 m	−4.06 m/s
	M03	105 m	11:38:25	−221 m	−4.05 m/s
	M04	105 m	11:40:04	−221 m	−4.08 m/s
S→R	M04	105 m	12:07:59	−112 m	4.05 m/s
	M03	105 m	12:09:37	−113 m	4.05 m/s
	M06	106 m	12:11:16	−114 m	4.05 m/s
R→S	M06	106 m	12:41:57	−107 m	−4.08 m/s
	M03	105 m	12:43:34	−116 m	−4.07 m/s
	M04	105 m	12:45:12	−105 m	−4.09 m/s

4

Estimation of the Alliance's Magnetic Dipole Moment

Assuming that the *Alliance* was sailing at constant speed along a straight line parallel to the line connecting the OBMs, 03, 04, and 06,we attempted to fit, in a least squares sense, a magnetic dipole, moving with the *Alliance*, to the observations. The mathematical formalism is described in Annex A.

In order to account for possible discrepancies between the nominal and actual positions of the OBMs, and between the magnetic centre and the GPS reference point of the *Alliance*, we shifted the measured against the modelled magnetic field in 1 s steps up to ±30 s (first two runs) and ±15 s (last four runs) from the nominal CPA and repeated the fitting procedure at each step. After each fit, we computed the difference between the measured magnetic field and the field that would result from the fitted magnetic dipole, for each vector component individually as well as for the total field. From the sum of squared differences between the expected and the observed absolute field we determined the root-mean-square (*rms*) errors.

The time shift which resulted in the minimum *rms* error for any given run and magnetometer was considered as marking the best-fit CPA (as opposed to the nominal CPA), of that particular OBM position. Applying a time shift is equivalent to displacing all OBMs by the same distance along a line parallel to the *Alliance* tracks.

In order to compensate for possible discrepancies between the nominal and actual OBM positions along a line perpendicular to the *Alliance* tracks, we repeated the procedure for the entire sequence of runs but with the OBMs displaced in steps of 4 m, toward as well as away from the *Alliance* tracks. We believe that the current drag on the modules during deployment is the main reason for their deviation from *Manning*'s GPS position. We chose to use identical displacements for the three OBMs, 03, 04 and 06, because they were deployed in less than one hour, and we assumed that the current pattern did not change significantly during that time interval.

We found the expected overall change in magnitude of the magnetic moment, corresponding to the fictitious change of OBM positions, but also a systematic difference between the minimum *rms* estimates obtained from different runs but using the

same OBM positions. We therefore imposed the constraint that we accept only solutions for which the total vertical and the permanent horizontal magnetic dipole moment do not vary systematically between runs made along different tracks. This constraint seems to be reasonable because, (i) the vertical axis of the *Alliance* had remained practically fixed with respect to the geomagnetic field for a long time before the test and (ii) the permanent magnetic moment remains constant by definition over time intervals of hours to days. We do not require that each of the two components of the horizontal permanent moment, along and perpendicular to the track, remain constant. Changing wind and current patterns can force the *Alliance* to sail with different yaw angles. This can result in an apparent variation of the longitudinal and perpendicular components of the permanent magnetic moments on purely geometrical grounds.

We initially applied the estimation procedure to the data from the last four runs only because they are not independent with respect to the OBM positions. Each OBM displacement affects on the estimates from all four runs. A northeastward displacement of the OBMs 03, 04 and 06 by 12 m (away from the *Alliance* tracks) results in a solution with minimum *rms* error which fulfills the constraints. We then applied a stepwise 4-m displacement of OBM 19 to the analysis of the first two runs and found that a southwestward displacement of OBM 19 by 12 m (i.e. also away from the *Alliance* track) results in a good match between the permanent horizontal and total vertical magnetic moments from the first two and the last four runs.

The minimum *rms* error varied vary little between the last four runs, it spanned 7% to 9% of the peak amplitude of the absolute magnetic field. For the first two runs, the *rms* error was larger, about 12% of the magnetic field peak amplitude. This might be due to the reduced speed of the *Alliance*, resulting in longer duration of the magnetic field distortion and possibly poorer low-frequency compensation for the effect of the sensor frequency response.

Figure 4 shows the *rms* errors for the last four runs after having applied a fictitious displacement to the OBMs 03, 04 and 06 of 12 m toward northeast. Figure 5 shows the results from the fitting procedure for the three OBMs for each of the last four runs. The top panel displays the results for the x-component of the magnetic moment, the center panel the y-component and the bottom panel the z-component. The circles mark those estimates which coincide with the smallest *rms* errors for each run and each OBM. They were considered representative for the *Alliance* magnetic dipole moment and are listed in Table 2 which includes the results from the first two runs not shown in Figs. 4 and 5.

The dipole moments obtained from reciprocating runs along parallel tracks permit differentiation between permanent and induced moments, at least in the horizontal plane. The permanent moment, fixed to the orientation of the ship, changes sign when the ship reverses her direction, while the induced magnetic moment re-

mains controlled by the geomagnetic field and thus fixed in direction. The following relations thus hold:

$$\begin{aligned} M_i^{(perm)} &= \frac{1}{2}\left(M_i^{(+)} - M_i^{(-)}\right) \\ M_i^{(ind)} &= \frac{1}{2}\left(M_i^{(+)} + M_i^{(-)}\right) \end{aligned} \tag{3}$$

with $i\epsilon\{x, y\}$. $M_i^{(+)}$ and $M_i^{(-)}$ denote magnetic moments obtained from runs in the positive and negative x directions, i.e. northwestward (e.g. B→A) and southeastward (e.g. A→B), respectively. No distinction between permanent and induced magnetic moment is possible in the vertical component as it is not practical to make a test run with the *Alliance* turned upside down.

Table 2 *Vector Components of the Magnetic Dipole Moment of RV Alliance*

Run ID	OBM	M_x [Am^2]	M_y [Am^2]	M_z [Am^2]	M_{abs} [Am^2]
B → A	M19	$130 \cdot 10^4$	$9 \cdot 10^4$	$87 \cdot 10^4$	$157 \cdot 10^4$
A → B	M19	$-77 \cdot 10^4$	$11 \cdot 10^4$	$88 \cdot 10^4$	$117 \cdot 10^4$
H → G	M04	$148 \cdot 10^4$	$32 \cdot 10^4$	$91 \cdot 10^4$	$176 \cdot 10^4$
	M03	$144 \cdot 10^4$	$30 \cdot 10^4$	$87 \cdot 10^4$	$171 \cdot 10^4$
	M06	$142 \cdot 10^4$	$30 \cdot 10^4$	$83 \cdot 10^4$	$167 \cdot 10^4$
G → H	M06	$-66 \cdot 10^4$	$39 \cdot 10^4$	$78 \cdot 10^4$	$109 \cdot 10^4$
	M03	$-61 \cdot 10^4$	$38 \cdot 10^4$	$84 \cdot 10^4$	$111 \cdot 10^4$
	M04	$-70 \cdot 10^4$	$44 \cdot 10^4$	$84 \cdot 10^4$	$119 \cdot 10^4$
S → R	M04	$151 \cdot 10^4$	$61 \cdot 10^4$	$85 \cdot 10^4$	$183 \cdot 10^4$
	M03	$142 \cdot 10^4$	$55 \cdot 10^4$	$87 \cdot 10^4$	$175 \cdot 10^4$
	M06	$144 \cdot 10^4$	$55 \cdot 10^4$	$81 \cdot 10^4$	$174 \cdot 10^4$
R → S	M06	$-63 \cdot 10^4$	$59 \cdot 10^4$	$86 \cdot 10^4$	$122 \cdot 10^4$
	M03	$-60 \cdot 10^4$	$54 \cdot 10^4$	$90 \cdot 10^4$	$121 \cdot 10^4$
	M04	$-72 \cdot 10^4$	$67 \cdot 10^4$	$90 \cdot 10^4$	$134 \cdot 10^4$

The magnetic dipole moments in Table 2 are plotted in Fig. 6. The time elapsed since 09:00 UTC on the day of the experiment serves as abscissa. Each estimate of the three components of the magnetic dipole moment is represented by three points at the corresponding time, red for the x-, blue for the y- and green for the z-component. Linear regression fits to the magnetic moments were computed separately for the northwestbound and the southeastbound runs, and a single regression line was fitted to the vertical moments.

A systematic variation over time of the horizontal components of the magnetic dipole moment (red and blue) is obvious while the vertical component (green) remains virtually constant over time. It is therefore not advisable to apply Eq. (3) to individual pairs of runs, such as the pair A→B abd B→A, which were performed at different times. We rather compute the permanent and induced magnetic moments directly from the regression lines, using the same equation, Eq. (3). The dashed lines represent the permanent magnetic moments and the dotted lines the induced moments.

The permanent horizontal magnetic moments remain constant over time. The permanent moment in starboard-port direction is close to zero, which is consistent with our expectations. The induced moments, however, increase monotonically over time. If we consider that the x- and y-axes of our coordinate system have a declination of $-45°$ and $+45°$, respectively, we find that the induced horizontal magnetic moment tends to increase with time. It is interesting to note that the induced perpendicular component (blue) increases at a higher rate than the induced longitudinal moment (red), irrespective of the shape of the *Alliance* which would favour the longitudinal direction because of its larger demagnetization factor, which is basically a form factor [2].

A further result can be obtained from the fitting procedure. The average time delay between passing the nominal CPAs and assuming the best fit is about 11.5 s for the northwestbound runs and some 4.5 s for the southeastbound runs (see also Fig. 4). It means that the *Alliance*, moving at a speed of 4.1 m/s, passed the actual CPAs some 19 m southeastward and some 47 m northeastward, respectively, of the nominal CPAs. The distance between the actual CPAs on opposite legs, (47+19)m=66m, suggests that the magnetic dipole moment of the *Alliance* is centred some 33 m astern of her GPS reference point.

The difference of about 7 s in the delays between up and down runs suggests that the actual OBM positions were about 15 m northwestward of the position of *Manning*'s GPS antenna during deployment. We thus conclude that the OBMs 03, 04 and 06 resided at a point about 15 m northwest and 12 m northeast of their nominal position, yielding a total positioning error of some 20 m.

When the same argument is applied to the first two runs we obtain best fits when the *Alliance* was past the nominal CPA by 8.5 s at the run B→A and short of the nominal CPA by 5.5 s at the run A→B. At speeds of 2.42 m/s and 2.57 m/s, respectively, this results in best fits for 21 m and 14 m, respectively, northwest of the nominal CPAs. We therefore suggest that the actual position of OBM 19 was 17-18 m northwest of its nominal position, in addition to the 12 m toward southwest derived before. However, in contradiction to our findings from above, these numbers are consistent with a distance of 3-4 m between the GPS reference point and the magnetic dipole centre of the *Alliance*.

We feel that OBM positioning errors of the order of 20 m, in a sea with a bottom depth of more than 100 m, mean a very precise deployment operation.

5
Conclusion

Figure 6 shows that the permanent magnetic dipole moment of the *Alliance* amounts to some 1,050,000 Am^2 along the stern-bow line and -30,000 Am^2 in starboard direction (i.e. it vanishes approximately) and has an undetermined contribution in vertical direction, up to a maximum of some 850,000 Am^2 (the latter number being valid if no induced vertical magnetic dipole moment existed). Thus the total permanent magnetic dipole moment of the *Alliance* lies between 1,050,000 Am^2 and 1,350,000 Am^2. One would expect a magnetic moment of some 1,200,000 Am^2 from a 3000-ton untreated ship, such as the *Alliance*.

There is no clear explanation of the steady increase of the induced horizontal magnetic moment.

Fluxgate magnetometers are known to be temperature-sensitive. However, temperature sensors in the magnetometer modules revealed that the temperature varied only by a small fraction of a degree over the duration of the experiment so that a change in sensitivity due to a change in ambient temperature can be excluded.

The four magnetometers used in the experiment were fully autonomous, neither connected to land nor to each other. All magnetometers showed unequivocally the variation of the induced horizontal magnetic dipole moment. An instrument degradation or failure can therefore be excluded. The fact that the horizontal components of $M^{(perm)}$ were constant supports the view that the instruments worked correctly.

A systematic change of orientation (yaw) of the *Alliance* between consecutive runs, necessitated for instance, by changing winds or water currents, can be excluded. Differences in deviation of the longitudinal axis from the –45°-line (changing yaw) should have been noticed as apparent changes of the permanent magnetic moment. An increase of one horizontal component of the magnetic moment as a result of a change in attitude of the *Alliance* should take place at the expense of the other horizontal component, whereas both horizontal components increased.

One could speculate that the induced magnetic moment of the *Alliance* has a medium-term memory, with the effect that it would build up over the four hours she was sailing predominantly in the same direction, namely along a –45°-line. This is consistent with the fact that the vertical moment did not change. We suggest

that both the permanent and the induced vertical moments, remained constant because the attitude of the *Alliance* with respect to its vertical axis remains constant irrespective of course.

The "misbehaviour" of the induced horizontal magnetic moment was unexpected, and the experiment was therefore not designed to study this effect. It would be desirable to perform a more systematic sea trial, covering a longer time interval, in order to investigate this effect.

6

Acknowledgements

I thank the SACLANTCEN technical staff for the preparation of the magnetometer modules, the *Manning* crew for the precise positioning of the modules during deployment, W. Zimmer for making DGPS navigation data available, and A. Magunia, a former SACLANTCEN summer research assistant, for conducting the magnetometer calibration measurements with extreme patience.

References

[1] Watermann, J, Lam, J., Distributions of magnetic field variations, differences and residuals, SACLANTCEN, SR-304, 1998.

[2] Sommerfeld, A., Vorlesungen über Theoretische Physik - Band 3: Elektrodynamik, reprint of the fourth edition, Harri Deutsch, Thun - Frankfurt/Main, 1977, p. 89.

[3] de Bruijn, A., Magnetic detection by a tri-axial magnetometer, SACLANTCEN, SM-233, 1990.

[4] Courant, R., Hilbert, D., Methods of Mathematical Physics, first English edition, Vol. I, Interscience, New York, 1953, p. 165

Annex A

Least-squares Solution for the Magnetic Dipole Moment

Let us assume that a ship (which may be a surface vessel or a submarine) sails with constant speed along a straight horizontal line. A coordinate system is defined such that its origin coincides with the position of a vector magnetometer fixed on the sea bottom. Its x-axis runs parallel to the track of the ship, its z-axis points vertically down, and its y-axis completes an orthogonal right-handed coordinate system.

Let h denote the vertical distance from the magnetometer to the ship and b the horizontal distance at its **P**oint of **C**losest **A**pproach (CPA). Let $r_0 = \sqrt{(h^2 + b^2)}$ be the corresponding range. Let v_0 denote the speed of the ship. These parameters are assumed to be known. We form a dimensionless time parameter, $\tau = t \cdot v_0 / r_0$, and we introduce the so-called "Anderson functions" (see [3])

$$\begin{aligned} A_0(\tau) &= (1+\tau^2)^{-5/2} \\ A_1(\tau) &= \tau\,(1+\tau^2)^{-5/2} \\ A_2(\tau) &= \tau^2\,(1+\tau^2)^{-5/2} \end{aligned} \tag{A1}$$

The three vector components of the magnetic field expected to be recorded by the magnetometer, $B_x^{(e)}(\tau)$, $B_y^{(e)}(\tau)$ and $B_z^{(e)}(\tau)$, can be expressed as

$$\begin{aligned} &\frac{4\pi r_0^3}{\mu_0} B_x^{(e)}(\tau) = \\ &\quad 2\,M_x\,A_2(\tau) + \frac{3}{r_0}\,(bM_y + hM_z)\,A_1(\tau) - M_x\,A_0(\tau) \\ &\frac{4\pi r_0^3}{\mu_0} B_y^{(e)}(\tau) = \\ &\quad -M_y\,A_2(\tau) + \frac{3b}{r_0} M_x\,A_1(\tau) + \left[\left(\frac{3b^2}{r_0^2} - 1\right) M_y + \frac{3bh}{r_0^2} M_z\right] A_0(\tau) \\ &\frac{4\pi r_0^3}{\mu_0} B_z^{(e)}(\tau) = \\ &\quad -M_z\,A_2(\tau) + \frac{3h}{r_0} M_x\,A_1(\tau) + \left[\frac{3bh}{r_0^2} M_y + \left(\frac{3h^2}{r_0^2} - 1\right) M_z\right] A_0(\tau) \end{aligned} \tag{A2}$$

These three equations are identical to Eq. (2.7a-c) of [3], with the only difference that the coordinate system has been changed and the terms reorganized. The change of the coordinate system requires proper consideration of the signs (i.e. h will always be negative). For a more detailed discussion on how to derive Eq. (A2) see [3].

For simplicity we introduce the parameter

$$k = \frac{4\pi r_0^3}{\mu_0} \tag{A3}$$

and the variables

$$\begin{aligned}
\alpha_x &= 2\,M_x \\
\beta_x &= \frac{3}{r_0}\,(bM_y + hM_z) \\
\gamma_x &= -M_x \\
\alpha_y &= -M_y \\
\beta_y &= \frac{3b}{r_0}\,M_x \\
\gamma_y &= \left[\left(\frac{3b^2}{r_0^2} - 1\right) M_y + \frac{3bh}{r_0^2}\,M_z\right] \\
\alpha_z &= -M_z \\
\beta_z &= \frac{3h}{r_0}\,M_x \\
\gamma_z &= \left[\frac{3bh}{r_0^2}\,M_y + \left(\frac{3h^2}{r_0^2} - 1\right) M_z\right]
\end{aligned} \tag{A4}$$

in order to write Eq. (A2) in the more convenient form

$$\begin{aligned}
k\,B_x^{(e)}(\tau) &= \alpha_x A_2(\tau) + \beta_x A_1(\tau) + \gamma_x A_0(\tau) \\
k\,B_y^{(e)}(\tau) &= \alpha_y A_2(\tau) + \beta_y A_1(\tau) + \gamma_y A_0(\tau) \\
k\,B_z^{(e)}(\tau) &= \alpha_z A_2(\tau) + \beta_z A_1(\tau) + \gamma_z A_0(\tau)
\end{aligned} \tag{A5}$$

Let $B_x^{(o)}$, $B_y^{(o)}$ and $B_z^{(o)}$ denote the three vector components of the observed magnetic field. It is our objective to fit the variables, $\alpha_x, \cdots, \gamma_z$, such that the expectations match the observations in a least squares sense. It means that we attempt to find numbers for the magnetic dipole moment components, M_x, M_y and M_z, such that the sum of squared differences between the expected and the actually observed magnetic field is minimal. The sum of squared differences, Q^2, (also termed the "residual sum of squares") reads

$$Q^2 = \sum_\tau (kB_x^{(o)} - kB_x^{(e)})^2 + \sum_\tau (kB_y^{(o)} - kB_y^{(e)})^2 + \sum_\tau (kB_z^{(o)} - kB_z^{(e)})^2 \qquad \text{(A6)}$$

Minimization of Q^2 means finding that set of nine variables, $\alpha_x, \cdots, \gamma_z$, which fulfills the conditions for making Q^2 a minimum. The latter, however, are not fully independent of each other because they are linear combinations of only three independent paremeters, M_x, M_y and M_z. Consequently, we have to find six relations which reduce the set of nine variables to three. A possible set of constraints, $g_1, \cdots, g_6$, can be obtained from Eq. (A4)

$$\begin{aligned}
0 = g_1 &= \alpha_x + 2\gamma_x \\
0 = g_2 &= \frac{3b}{r_0}\alpha_x - 2\beta_y \\
0 = g_3 &= \frac{3h}{r_0}\alpha_x - 2\beta_z \\
0 = g_4 &= \beta_x + \frac{3b}{r_0}\alpha_y + \frac{3h}{r_0}\alpha_z \\
0 = g_5 &= \gamma_y + \left(\frac{3b^2}{r_0^2} - 1\right)\alpha_y + \frac{3bh}{r_0^2}\alpha_z \\
0 = g_6 &= \gamma_z + \frac{3bh}{r_0^2}\alpha_y + \left(\frac{3h^2}{r_0^2} - 1\right)\alpha_z
\end{aligned} \qquad \text{(A7)}$$

We now reformulate the minimization problem using Lagrange's method of multipliers [4],

$$P = Q^2 + \sum_{i=1}^{6} \lambda_i g_i \stackrel{!}{=} min \qquad \text{(A8)}$$

which treats the 15 variables, $\alpha_x, \cdots, \gamma_z, \lambda_1, \cdots, \lambda_6$, as independent, and solve the minimization problem with respect to these 15 variables. That means we solve the rank-15 system of linear equations

$$\begin{aligned}
\frac{\partial P}{\partial \alpha_x} = 0\,, \quad \cdots \quad \frac{\partial P}{\partial \gamma_z} = 0 \\
\frac{\partial P}{\partial \lambda_1} = 0\,, \quad \cdots \quad \frac{\partial P}{\partial \lambda_6} = 0
\end{aligned} \qquad \text{(A9)}$$

The partial derivatives are obtained from Eq. (A6) in connection with Eq. (A7), and read

$$
\begin{aligned}
\frac{\partial P}{\partial \alpha_x} &= -2\sum_\tau A_2(kB_x^{(o)} - \alpha_x A_2 - \beta_x A_1 - \gamma_x A_0) + \lambda_1 + \frac{3b}{r_0}\lambda_2 + \frac{3h}{r_0}\lambda_3 \\
\frac{\partial P}{\partial \beta_x} &= -2\sum_\tau A_1(kB_x^{(o)} - \alpha_x A_2 - \beta_x A_1 - \gamma_x A_0) + \lambda_4 \\
\frac{\partial P}{\partial \gamma_x} &= -2\sum_\tau A_0(kB_x^{(o)} - \alpha_x A_2 - \beta_x A_1 - \gamma_x A_0) + 2\lambda_1 \\
\frac{\partial P}{\partial \alpha_y} &= -2\sum_\tau A_2(kB_y^{(o)} - \alpha_y A_2 - \beta_y A_1 - \gamma_y A_0) + \frac{3b}{r_0}\lambda_4 + \left(\frac{3b^2}{r_0^2} - 1\right)\lambda_5 + \frac{3bh}{r_0^2}\lambda_6 \\
\frac{\partial P}{\partial \beta_y} &= -2\sum_\tau A_1(kB_y^{(o)} - \alpha_y A_2 - \beta_y A_1 - \gamma_y A_0) - 2\lambda_2 \\
\frac{\partial P}{\partial \gamma_y} &= -2\sum_\tau A_0(kB_y^{(o)} - \alpha_y A_2 - \beta_y A_1 - \gamma_y A_0) + \lambda_5 \\
\frac{\partial P}{\partial \alpha_z} &= -2\sum_\tau A_2(kB_z^{(o)} - \alpha_z A_2 - \beta_z A_1 - \gamma_z A_0) + \frac{3h}{r_0}\lambda_4 + \frac{3bh}{r_0^2}\lambda_5 + \left(\frac{3h^2}{r_0^2} - 1\right)\lambda_6 \\
\frac{\partial P}{\partial \beta_z} &= -2\sum_\tau A_1(kB_z^{(o)} - \alpha_z A_2 - \beta_z A_1 - \gamma_z A_0) - 2\lambda_3 \\
\frac{\partial P}{\partial \gamma_z} &= -2\sum_\tau A_0(kB_z^{(o)} - \alpha_z A_2 - \beta_z A_1 - \gamma_z A_0) + \lambda_6 \\
\frac{\partial P}{\partial \lambda_1} &= \alpha_x + 2\gamma_x \\
\frac{\partial P}{\partial \lambda_2} &= \frac{3b}{r_0}\alpha_x - 2\beta_y \\
\frac{\partial P}{\partial \lambda_3} &= \frac{3h}{r_0}\alpha_x - 2\beta_z \\
\frac{\partial P}{\partial \lambda_4} &= \beta_x + \frac{3b}{r_0}\alpha_y + \frac{3h}{r_0}\alpha_z \\
\frac{\partial P}{\partial \lambda_5} &= \gamma_y + \left(\frac{3b^2}{r_0^2} - 1\right)\alpha_y + \frac{3bh}{r_0^2}\alpha_z \\
\frac{\partial P}{\partial \lambda_6} &= \gamma_z + \frac{3bh}{r_0^2}\alpha_y + \left(\frac{3h^2}{r_0^2} - 1\right)\alpha_z
\end{aligned}
\qquad \text{(A10)}
$$

The system of 15 linear equations in the 15 variables, $\alpha_x, \cdots, \gamma_z, \lambda_1, \cdots, \lambda_6$, is solved using standard methods of numerical mathematics. The first terms of the left-hand side of Eq. (A10), $\sum_\tau A_i k B_j$ with $i\epsilon\{0,1,2\}$ and $j\epsilon\{x,y,z\}$ represent the inhomogenous terms of the system of equations.

The solution of the system yields immediately the three components of magnetic dipole moment (see Eq. (A4)):

$$\begin{aligned} M_x &= -\gamma_x \\ M_y &= -\alpha_y \\ M_z &= -\alpha_z \end{aligned} \tag{A11}$$

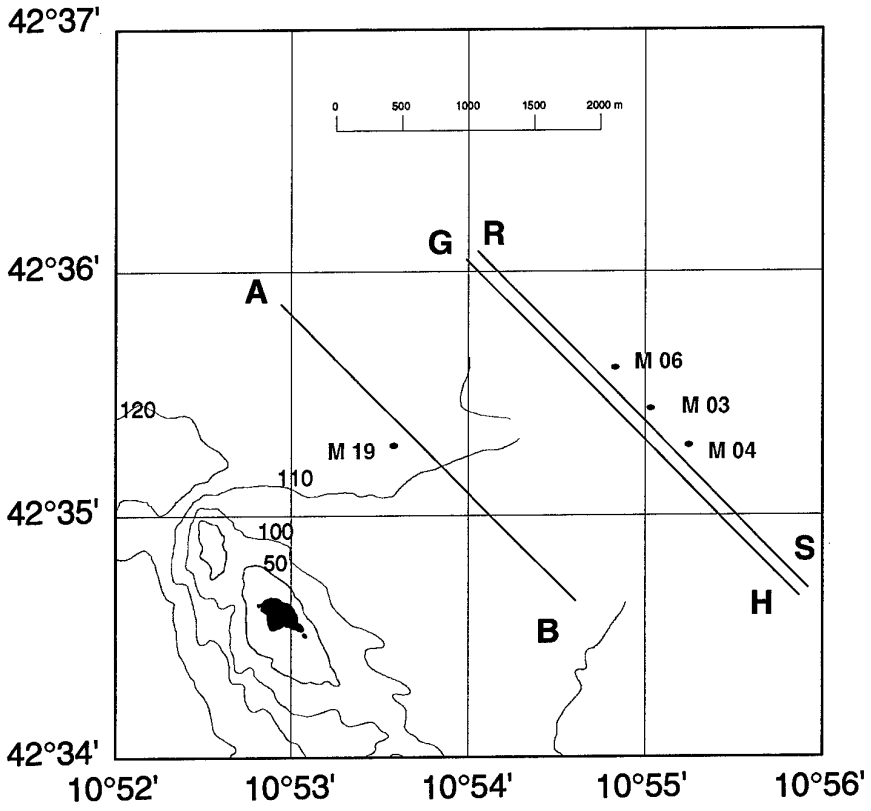

Figure 1: *Map of the test site northwest of Formica Grande di Grosseto. M03, M04, M06 and M19 denote the Ocean Bottom Magnetometers in operation during the test. The dots mark their positions. The lines A-B, G-H and R-S mark the tracks followed by the Alliance during the test runs.*

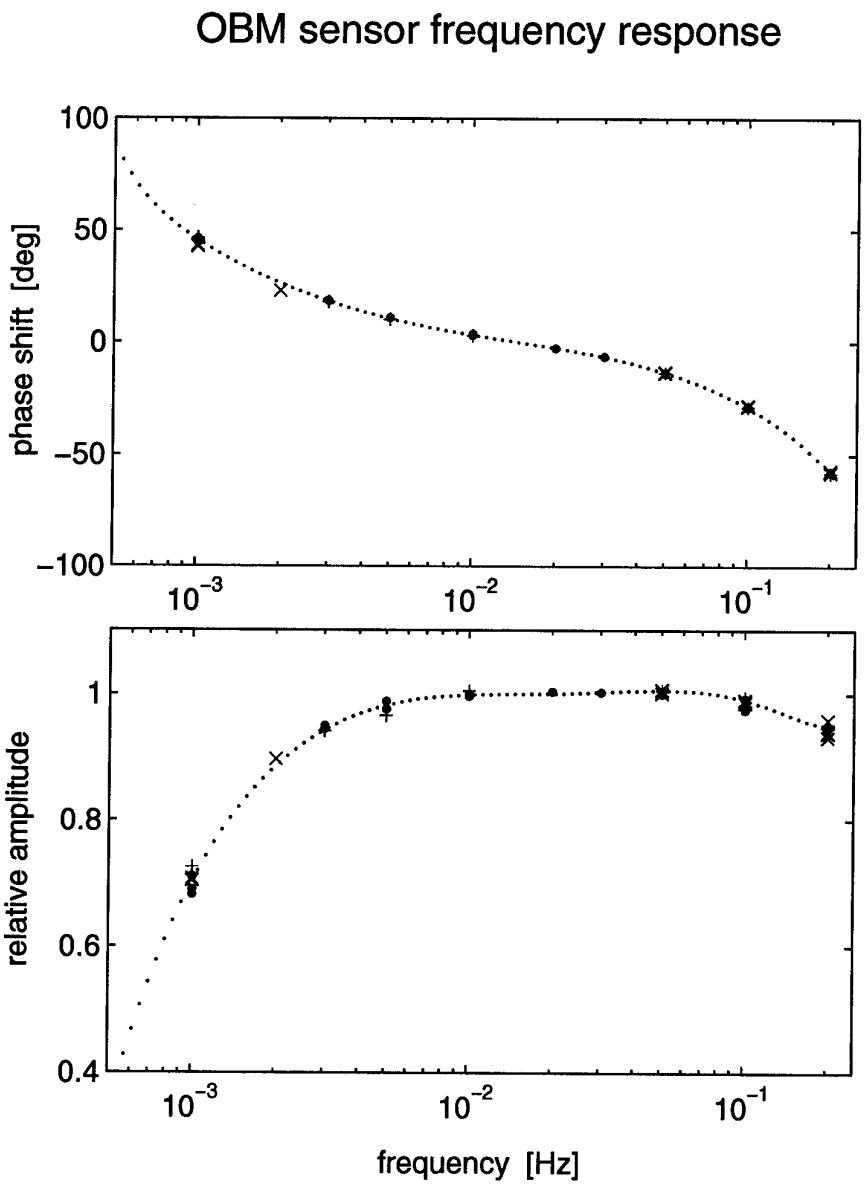

Figure 2: *Measurements of the sensor requency response and best-fitting polynomials of order 5 (markers and dotted lines, respectively), from two different magnetometers. Each marker represents the measurement from one vector component of one OBM. The amplitudes were normalized to 15 mHz (where the phase shift becomes zero). The amplitude scaling factor at 15 mHz is ±100 nT for the full range of the ADC.*

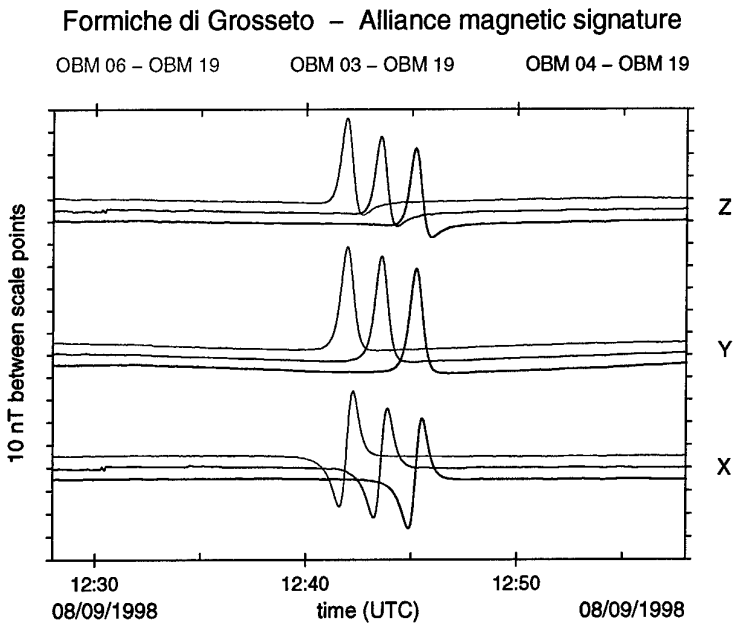

Figure 3: *Magnetic signature of RV Alliance recorded by M03, M04 and M06 during a run from R to S (see Fig. 1), corrected for the sensor frequency response and compensated for spatially uniform magnetic field variations using M19 as reference. From top to bottom: magnetic field components in vertical, northeast and northwest direction. For better graphical distinction, different vertical offsets were applied to the individual curves*

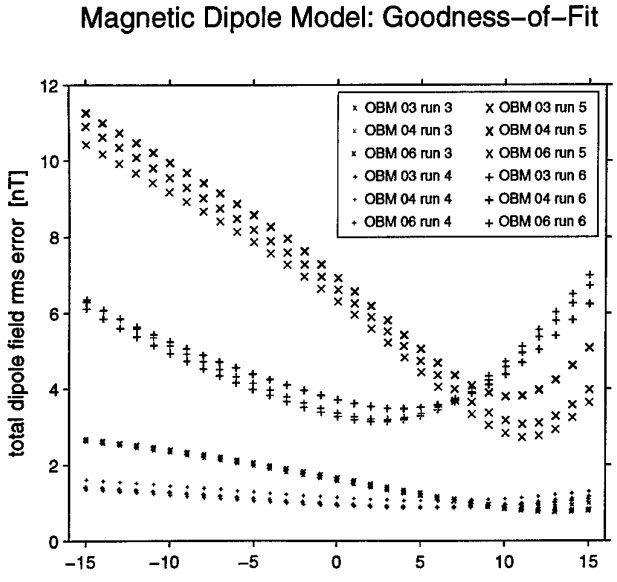

Figure 4: *Root-mean-square differences between measured magnetic fields and those expected from a magnetic dipole moving with the Alliance. Starting from the nominal closest point of approach, a sequence of dipoles was fitted to the observations, delaying and advancing the nominal closest point of approach by 1 s at each step. Results from runs 3-6, computed for a fictitious northeastward displacement of the OBMs by 12 m, are shown here.*

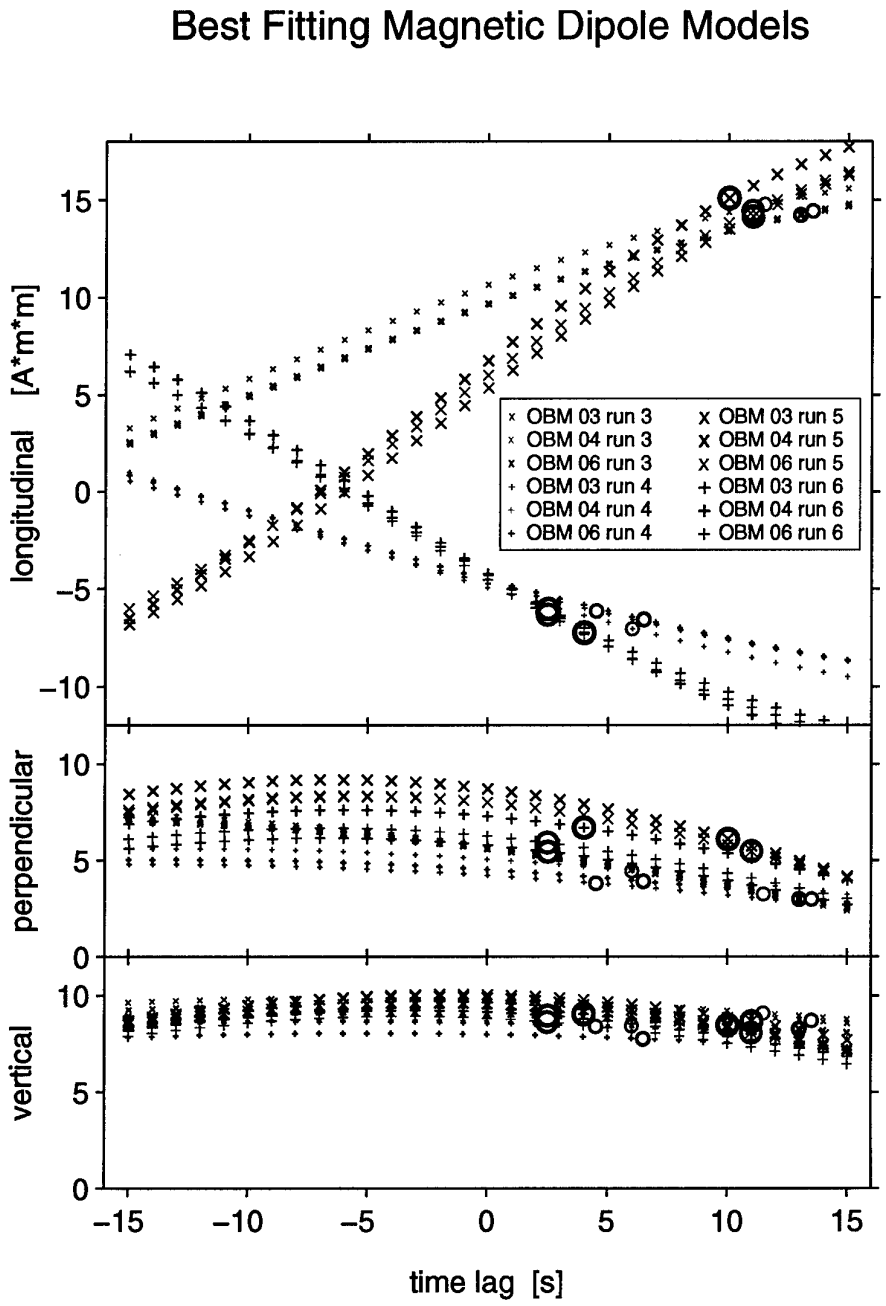

Figure 5: *Magnetic dipole moments along the fore and aft line (top panel), athwartships (centre panel) and vertical (bottom panel) for the same runs and magnetometers and the same time steps and displacement as in Fig. 4. The advanced or delayed closest points of approach which resulted in the minimum rms errors are emphasized by circles.*

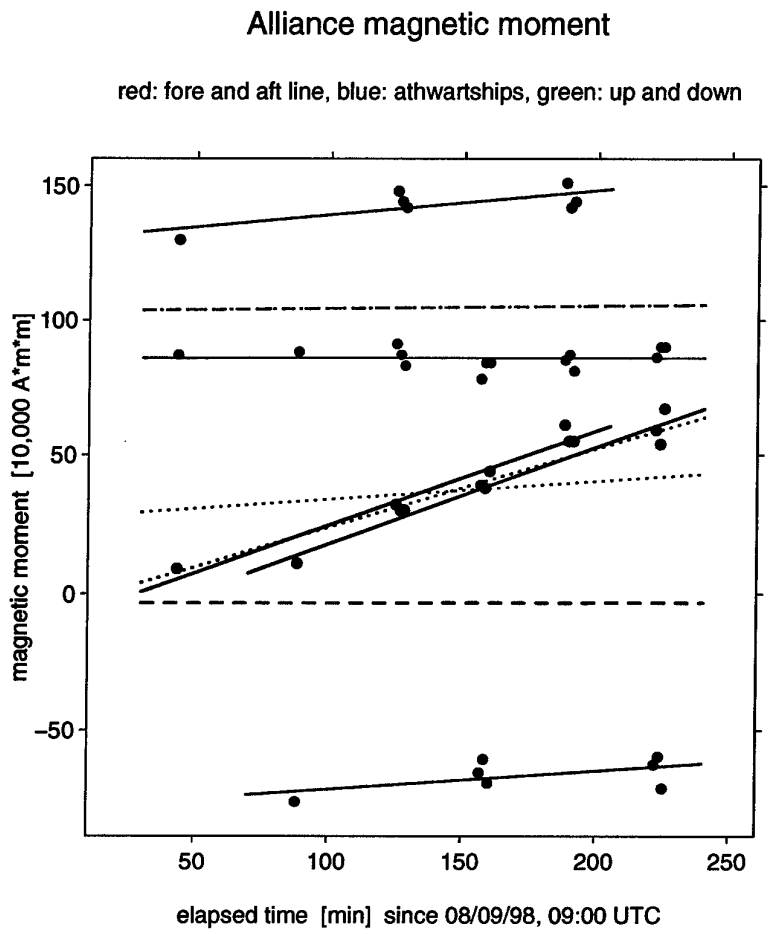

Figure 6: *Estimated magnetic dipole moments over elapsed experiment time. The dots correspond to the circles in Figure 5. Orientations are colour-coded, red: longitudinal, blue: perpendicular, green: vertical. Solid lines: linear regression of the horizontal dipole moments, separately for northwestbound and southeastbound runs, and of the combined vertical dipole moments. Dashed lines: permanent part of the horizontal dipole moments; dotted lines: induced part of the horizontal dipole moments.*

Document Data Sheet

NATO UNCLASSIFIED

Security Classification		Project No.
UNCLASSIFIED		06-A
Document Serial No.	**Date of Issue**	**Total Pages**
SR-312	February 1999	30 pp.

Author(s)

Watermann, J.

Title

The magnetic dipole moment of RV *Alliance*

Abstract

A SACLANTCEN magnetometry sea trial was performed in September 1998 in the northern Tyrrhenian Sea in the vicinity of the Formiche di Grosseto islands. One of the trial objectives concerned the measurement of the magnetic dipole moment of the NATO research vessel *Alliance* with an array of fixed Ocean Bottom Magnetometers. The *Alliance* sailed with constant velocity along three specified tracks in reciprocating directions. The magnetic signature of the *Alliance* was subsequently extracted from the magnetic field data recorded during the experiment. From the magnetic signatures taken from six successive runs, quantitative magnetic dipole models were derived. A comparison between the magnetic signatures obtained from northwestward and southeastward runs yields estimates of the permanent and induced magnetic dipole moments in the horizontal plane. In the vertical direction, only the total magnetic dipole moment can be determined. The positions of the OBMs, uncertain to some extent, were fictitiously varied such that the horizontal components of the permanent magnetic dipole moment and the vertical component of the total dipole moment remained constant during the experiment. The induced horizontal dipole moment tended to increase steadily and monotonically in a northward direction. Explanations of this phenomenon are discussed.

Keywords

Issuing Organization

North Atlantic Treaty Organization
SACLANT Undersea Research Centre
Viale San Bartolomeo 400, 19138 La Spezia, Italy

[From N. America: SACLANTCEN (New York) APO AE 09613]

Tel: +39 0187 527 361
Fax:+39 0187 524 600

E-mail: library@saclantc.nato.int

NATO UNCLASSIFIED

Initial Distribution for SR-312

Ministries of Defence

DND Canada	10
CHOD Denmark	8
MOD Germany	15
HNDGS Greece	12
MARISTAT Italy	9
MOD (Navy) Netherlands	12
NDRE Norway	10
MOD Portugal	5
MDN Spain	2
TDKK and DNHO Turkey	5
MOD UK	20
ONR USA	32

NATO Commands and Agencies

NAMILCOM	2
SACLANT	3
CINCEASTLANT/ COMNAVNORTHWEST	1
CINCIBERLANT	1
CINCWESTLANT	1
COMASWSTRIKFOR	1
COMSTRIKFLTANT	1
COMSUBACLANT	1
SACLANTREPEUR	1
SACEUR	2
CINCNORTHWEST	1
CINCSOUTH	1
COMEDCENT	1
COMMARAIRMED	1
COMNAVSOUTH	1
COMSTRIKFORSOUTH	1
COMSUBMED	1
NC3A	1
PAT	1

Scientific Committee of National Representatives

SCNR Belgium	1
SCNR Canada	1
SCNR Denmark	1
SCNR Germany	1
SCNR Greece	1
SCNR Italy	1
SCNR Netherlands	2
SCNR Norway	1
SCNR Portugal	1
SCNR Spain	1
SCNR Turkey	1
SCNR UK	1
SCNR USA	2
SECGEN Rep. SCNR	1
NAMILCOM Rep. SCNR	1

National Liaison Officers

NLO Canada	1
NLO Denmark	1
NLO Germany	1
NLO Italy	1
NLO Netherlands	1
NLO Spain	1
NLO UK	1
NLO USA	1

Sub-total	188
SACLANTCEN	30
Total	218